(^{t}BuN≡C)$_2$Ni(C_2H_2) (19). The red solution of 816.5 mg (1.0 mmol) of $Ni_4(^t$BuNC)$_7$ in 20 mL of ether (obtained and filtrated at 20 °C) is cooled to −50 °C. Upon addition of 83.1 mg (1.0 mmol) of ^{t}BuNC and about 150 mL (6 mmol) of ethyne, the red lightens slightly. After a few minutes yellow-brownish needles form, which are separated from the mother liquor, washed twice with cold pentane, and dried in vacuo: yield 622 mg (62%); above 0 °C dec. ^{1}H NMR (THF-d_8, −30 °C): δ 6.57 (C_2H_2), 1.45 (CH_3). ^{13}C NMR (THF-d_8, −30 °C): δ 157.5 (N≡C), 115.2 (d, J(CH) = 212 Hz, C_2H_2), 56.25 (CMe_3), 30.7 (CH_3). Anal. Calcd for $C_{12}H_{20}N_2Ni$ (251.0): C, 57.42; H, 8.03; N, 11.16; Ni, 23.39. Found: C, 57.60; H, 7.58; N, 11.38; Ni, 23.44.

Acknowledgment. I thank A. Manhart and E. Rickers for experimental help, Drs. R. Benn (^{1}H NMR), R. Mynott (^{13}C, ^{31}P NMR), and K. Seevogel (IR) of this institute for spectroscopic studies, and Prof. G. Wilke for his continued interest in this work.

Organometallic Photochemistry in Thin Polymeric Films. Photoimaging

Terrence R. O'Toole, B. Patrick Sullivan, and Thomas J. Meyer*

Contribution from the Department of Chemistry, University of North Carolina at Chapel Hill, Chapel Hill, North Carolina 27599-3290. *Received April 11, 1988*

Abstract: Dark green polymeric films of poly[(vbpy)Re(CO)$_3$]$_2$ have been prepared on electrode surfaces by reductive electropolymerization of [(vbpy)Re(CO)$_3$Cl]. Visible photolysis of the films immersed in CCl_4 leads to the cleavage of the metal–metal bond and formation of yellow poly[(vbpy)Re(CO)$_3$Cl] by photochemically well-defined processes. On the basis of the photochemistry, yellow-on-green images can be created in the films. They can be erased in a subsequent electrochemical reduction step, which re-forms the green dimer in 70% yield. The images can be developed further by allowing the unreacted dimer to react with appropriate organic oxidants or with Ag^+, which leads to the deposition of metallic silver in the dark areas of a light-generated pattern. Further deposition of silver can be carried out selectively in these unexposed regions by electrochemical reduction of Ag^+ in an external solution.

We report here the preparation and photochemical properties of electrode-bound, thin polymeric films in which there are molecular units containing metal-to-metal bonds. A goal of the work was to develop a reversible photoimaging system based on a well-established metal–metal bond cleavage reaction in solution (eq 1).[1,2] The underlying strategy was to combine photochemically

$$(CO)_5MnMn(CO)_5 \overset{h\nu}{\rightleftharpoons} 2Mn(CO)_5^{\bullet} \xrightarrow{CCl_4} 2Mn(CO)_5Cl \quad (1)$$

$$2Mn(CO)_5Cl \xrightarrow{2e^-} Mn_2(CO)_{10} + 2Cl^- \quad (2)$$

induced halogen abstraction with electrochemical reduction (eq 2) as a means of returning the system to the metal–metal bonded state. We felt that a combination of the two, but in the translationally restricted environment of a polymeric film, could provide the basis for a sequential photochemical–electrochemical write–erase cycle.

The system chosen for study was a film-based analogue of [(bpy)Re(CO)$_3$Cl] (bpy is 2,2′-bipyridine). In earlier work it was shown that well-defined films of poly[(vbpy)Re(CO)$_3$Cl] (vbpy

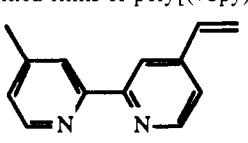

(vbpy)

is 4-methyl-4′-vinyl-2,2′-bipyridine) can be formed on electrode surfaces[3] by using what are, by now, standard reductive electropolymerization techniques.[4] In the earlier work it was shown that many of the chemical and physical properties of the metal complex sites are retained in the film environment. In addition, polymeric films containing the metal–metal bonded dimer, poly[(vbpy)-Re(CO)$_3$]$_2$, can be prepared by further electrochemical reduction of poly[(vbpy)Re(CO)$_3$Cl].

Experimental Section

The electropolymerization and electrochemical experiments and some of the photochemical experiments were carried out in a Vacuum/Atmospheres glovebox with a slow, continuous flow of fresh nitrogen.

Materials. Acetonitrile (Burdick and Jackson, UV-grade, distilled in glass) and methylene chloride (Aldrich, Gold Label) were opened and stored in the glovebox and used as received. Small amounts (~20 mL) of carbon tetrachloride (Fisher) and 1,2-difluorobenzene (Aldrich, 98%) were purged with N_2 before being sealed and brought into the glovebox. Both carbon tetrachloride and 1,2-difluorobenzene (DFB) were purified by passage down a column of activated alumina. Tetra-*n*-butylammonium hexafluorophosphate (TBAH) was precipitated from water by mixing aqueous solutions containing stoichiometric amounts of tetra-*n*-butylammonium bromide and KPF_6 (both from Aldrich). The resulting precipitate was recrystallized twice from ethanol, dissolved in a minimum amount of acetonitrile, filtered to remove solid impurities, and precipitated into ether. The resulting white solid was washed with ether and dried in vacuo at 50 °C for 78 h. The syntheses of *fac*-[(vbpy)Re(CO)$_3$Cl],[3] [(bpy)Re(CO)$_3$]$_2$[5a] (bpy is 2,2′-bipyridine), and [(4,4′-dmbpy)Re(CO)$_3$]$_2$[5b] (4,4′-dmbpy is 4,4′-dimethyl-2,2′-bipyridine) are reported elsewhere. $AgPF_6$, 2,3-dichloro-5,6-dicyano-1,4-benzoquinone

(1) (a) Wrighton, M. S.; Bredesen, D. *J. Organomet. Chem.* **1973**, *50*, C35. (b) Wrighton, M. S.; Ginley, D. S. *J. Am. Chem. Soc.* **1975**, *97*, 2065.
(2) Meyer, T. J.; Caspar, J. V. *Chem. Rev.* **1985**, *85*, 187.
(3) (a) O'Toole, T. R.; Margerum, L. D.; Westmoreland, T. D.; Vining, W. J.; Murray, R. W.; Meyer, T. J. *J. Chem. Soc., Chem. Commun.* **1985**, 1416. (b) Cabrera, C. R.; Abruña, H. D. *J. Electroanal. Chem., Interfacial Electrochem.* **1986**, *209*, 101. (c) O'Toole, T. R.; Margerum, L. D.; Bruce, M. R.; Sullivan, B. P.; Murray, R. W.; Meyer, T. J. *J. Electroanal. Chem., Interfacial Electrochem.* **1989**, *259*, 217.
(4) (a) Abruña, H. D.; Denisevich, P.; Umana, M.; Meyer, T. J.; Murray, R. W. *J. Am. Chem. Soc.* **1981**, *103*, 56. (b) Denisevich, P.; Abruña, H. D.; Leidner, C. R.; Meyer, T. J.; Murray, R. W. *Inorg. Chem.* **1982**, *21*, 2153. (c) Leidner, C. R.; Sullivan, B. P.; Reed, R. A.; White, B. A.; Crimmins, M. T.; Murray, R. W.; Meyer, T. J. *Inorg. Chem.* **1987**, *26*, 882. (d) Sullivan, B. P.; Meyer, T. J.; Caspar, J. V. *Inorg. Chem.* **1987**, *26*, 4145.
(5) (a) Sullivan, B. P.; Bolinger, C. M.; Conrad, D.; Vining, W. J.; Meyer, T. J. *J. Chem. Soc., Chem. Commun.* **1985**, 1414. (b) Abruña, H. D.; Breikss, A. *J. Electroanal. Chem., Interfacial Electrochem.* **1986**, *201*, 347. (c) Sullivan, B. P.; Bruce, M. R.; O'Toole, T. R.; Bolinger, C. M.; Megehee, E. B.; Thorp, H.; Meyer, T. J. In *Catalytic Activation of Carbon Dioxide*; Ayers, W. M., Ed.; ACS Symposium Series 363; American Chemical Society: Washington, DC 1988; pp 52–90. (d) O'Toole, T. R.; Sullivan, B. P.; Meyer, T. J., to be submitted for publication.

0002-7863/89/1511-5699$01.50/0

(DDQ), 7,7,8,8-tetracyanoquinodimethane (TCNQ) (Aldrich), $Co^{II}(pc)$ (pc is phthalocyanine) (Kodak), and other reagents and solvents were

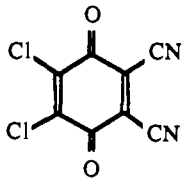

DDQ

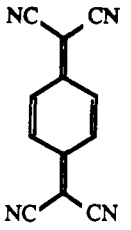

TCNQ

ACS grade or better and were used as received. The structures of the two organic oxidants and the metal complex are shown above and below. The oxidized form of the complex, $[Co^{III}(pc)(CH_3CN)_2]^+$, was generated in CH_3CN by partial oxidation of suspended $[Co^{II}(pc)]$ with a limiting amount of ceric ammonium nitrate.

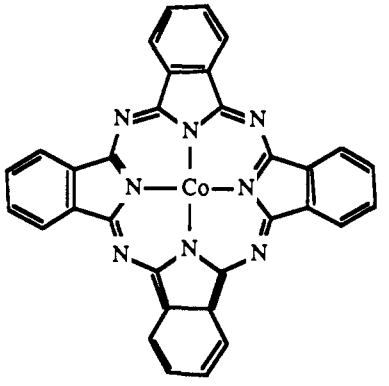

Co(pc)

Electrochemistry. Optically transparent electrodes (OTEs) of indium-doped tin oxide (ITO) on glass (Delta Technologies) were used for UV–visible spectroscopic studies. The conductive surface was cleaned before use by immersion in concentrated HNO_3 (~2 min) followed by rinsing with water and methanol. Platinum and glassy-carbon electrodes of area ~0.1 cm^2 seated in Teflon shrouds were used for routine electrochemical measurements and surface analyses. They were cleaned by polishing with 1-μm diamond paste (Buehler), followed by rinsing with water and methanol. Electrochemical measurements were performed by using a PAR Model 273 potentiostat with a Hewlett-Packard Model 5017B X-Y recorder. All electrochemical potentials were referenced to a saturated sodium chloride calomel electrode (ssce). Three-compartment cells were employed where the reference and auxiliary electrodes were separated from the working electrode with fine- and medium-porosity glass frits, respectively.

Films of poly[(vbpy)$Re(CO)_3]_2$ were prepared on electrode surfaces by two methods. In method 1 the potential of a freshly cleaned electrode was cycled between −0.85 and −1.85 V at 100 mV/s in a 0.1 M TBAH/CH_3CN solution containing ~5 mM [(vbpy)$Re(CO)_3Cl$]. The surface coverage of poly[(vbpy)$Re(CO)_3]_2$ (Γ_{Re_2}) increases with the number of cycles although not in a linear fashion. Between 5 and 40 cycles were typically required to generate films with $\Gamma_{Re_2} \sim (1-6) \times 10^{-8}$ mol/cm^2.

In method 2 a polymeric film of poly[(vbpy)$Re(CO)_3Cl$] was first grown on an electrode under the same conditions as above by using either CH_3CN or 1,2-difluorobenzene (DFB)[6] as solvent but limiting the reductive scan to −1.6 V. Subsequent reduction to the Re–Re bond was accomplished by two additional reductive scans between −0.85 and −2.0 V in a fresh 0.1 M TBAH/DFB (or CH_3CN) solution. Films prepared by this sequential technique were used in the kinetic and surface analysis studies. Potentials more positive than ~−0.4 V must be avoided during these procedures because the dimeric sites in the films undergo irreversible oxidation at $E_{p,a} = -0.15$ V.

Photochemistry and Spectroscopy. A Hewlett-Packard Model 8451A diode array spectrophotometer was used to record routine electronic spectra. A computerized Cary 14 (On-Line Instruments Co.) was used to record spectra that extend into the near IR. Photochemical kinetics were followed by monitoring the spectral changes that occur with time following 436-, 540-, or 580-nm irradiation of films of poly[(vbpy)$Re(CO)_3]_2$ on ITO electrodes. which were immersed in O_2-free CCl_4. The monitoring wavelengths were at 630 or 845 nm, which are λ_{max} values for poly[(vbpy)$Re(CO)_3]_2$. The light intensity at 436 nm was measured by ferrioxalate actinometry[7] and the intensities at 540 and 580 nm relative to that at 436 nm by using a Scientech 365 power meter. The optical train consisted of a Bausch and Lomb Model SP 200 mercury lamp, the output of which passed through a Bausch and Lomb Model 33-86-02 monochromator of band-pass ±10 nm. The light source for qualitative experiments was either sunlight or a 175-W sunlamp passed through a No. 5-57 Bausch and Lomb blue filter, which isolated the irradiation range 350–550 nm.

Film absorption spectra were complicated by sloping backgrounds, which arise from light scattering. The effect increases with film thickness and incident light energy. In order to account for light scattering, comparisons were made between films of poly[(vbpy)$Re(CO)_3]_2$ and CH_3CN solutions containing [(4,4′-dmbpy)$Re(CO)_3]_2$, which were of approximately equal absorbance. A base line free of light-scattering effects was estimated by matching the solution and film spectra at long wavelengths where light scattering is negligible and taking the difference between the two at shorter wavelengths.

Photoimaging. Light-generated images were created by photolysis of poly[(vbpy)$Re(CO)_3]_2$ on optically transparent electrodes. The film-coated electrodes were placed in a thin-glass cell with a mask painted on the external surface. Carbon tetrachloride was added, and the cell was photolyzed. The reactions were complete after an exposure time of ~30 s with filtered sunlight or 5–10 min with the sunlamp.

Reactions between the poly[(vbpy)$Re(CO)_3]_2$ sites in the films and Ag^+, TCNQ, DDQ, or $[Co^{III}(pc)(CH_3CN)_2]^+$ were carried out by immersing electrodes into CH_3CN solutions, which were ~0.01 M in oxidant. The reactions were complete within a few seconds for Ag^+ and the organic oxidants and within 1 min for the Co(III) oxidant.

In order to explore spatial resolution, a line pattern was generated by passing a laser beam (Spectra Physics 164 Ar laser with Spectra Physics 265 Exciter) through a diffraction grating (100 lines/in.). Appropriate lenses were used to expand and refocus the line pattern to the desired size. The excitation wavelength was 457.9 nm, and the beam power was ~5 mW.

Surface Analysis. A combination scanning electron microscope (ISI DS-130) and energy-dispersive X-ray spectrometer (Tracor Northern TN-5500 EDS) was used to characterize the surface structure and elemental composition of polymeric films on glassy-carbon or Pt electrodes. An electron beam energy of 5 keV was used in most of the experiments.

Results

Electrochemistry. Reductive electropolymerization of [(vbpy)$Re(CO)_3Cl$] in 0.1 M TBAH/CH_3CN solutions by negative potential scans to potentials more positive than −1.6 V (vs ssce) gives yellow films of poly[(vbpy)$Re(CO)_3Cl$].[3] The growth of poly[(vbpy)$Re(CO)_3Cl$] through a series of reductive scans in DFB is shown in the cyclic voltammograms in Figure 1A. In earlier work it was shown that these films retain the spectroscopic (XPS,[3a,c] IR,[3c] and UV–vis[3]) and at least some of the chemical properties of [(bpy)$Re(CO)_3Cl$] in solution. The latter includes the ability to act as an electrocatalyst for the reduction of CO_2 to CO.[3] Green films of poly[(vbpy)$Re(CO)_3]_2$ can be prepared in a subsequent step by reducing poly[(vbpy)$Re(CO)_3Cl$] films in potential scans that are extended to −1.7 V or to potentials more negative (eq 3).[3b,c] The electrogeneration of poly[(vbpy)Re-

$$2\text{poly[(vbpy)Re(CO)}_3\text{Cl]} + 2e^- \rightarrow \text{poly[(vbpy)Re(CO)}_3]_2 + 2Cl^- \quad (3)$$

$(CO)_3]_2$ from poly[(vbpy)$Re(CO)_3Cl$] is consistent with the electrochemistry observed for [(bpy)$Re(CO)_3Cl$] in CH_3CN.[5] In solution, reduction of [(bpy)$Re(CO)_3Cl$] occurs to give [(bpy)-$Re(CO)_3Cl]^-$ ($E_{1/2} = -1.33$ V), which is followed by relatively slow loss of Cl^- and coupling to give [(bpy)$Re(CO)_3]_2$.[5] Reduction past −1.7 V results in the rapid loss of Cl^- and formation of the anion, $[(bpy)Re(CO)_3]^-$, which dimerizes upon reoxidation. As for [(bpy)$Re(CO)_3]_2$ in solution, the metal–metal bond in poly-[(vbpy)$Re(CO)_3]_2$ undergoes a further, irreversible oxidation to the corresponding acetonitrilo complex, poly[(vbpy)$Re(CO)_3$-

(6) O'Toole, T. R.; Younathan, J. N.; Sullivan, B. P.; Meyer, T. J. *Inorg. Chem.*, in press.

(7) Calvert, J. G.; Pitts, J. N. Photochemistry; Wiley: New York, 1967.

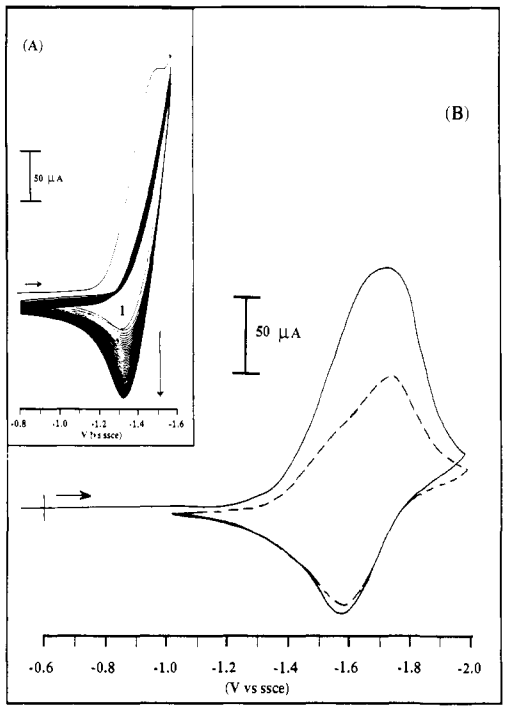

Figure 1. (A) Successive cyclic voltammograms in a solution containing ~5 mM [(vbpy)$Re(CO)_3Cl$] in 0.1 M TBAH/DFB at an ITO electrode. The first scan is labeled. (B) Cyclic voltammograms of the film formed in (A) in fresh 0.1 M TBAH/DFB at 50 mV/s. The solid line (—) is the first scan, and the dashed line (- - -) is the second scan.

$(CH_3CN)]^+$, if oxidative scans are extended to or past −0.15 V.

As shown in Figure 1B, an initial reductive scan of poly-[(vbpy)$Re(CO)_3Cl$] to −2.0 V results in a 2e reduction. The product is the dark purple anion poly[(vbpy)$Re(CO)_3]^-$, which forms with loss of Cl^- from the film. On the return scan, dimerization occurs following a net 1e oxidation of poly[(vbpy)-$Re(CO)_3]^-$. The second sweep (dashed line) shows the characteristic two-wave reduction pattern that has been observed for [(bpy)$Re(CO)_3]_2$ in solution.[5d] Consecutive scans between −1.0 and −2.0 V show little change from the dashed voltammogram if DFB is used as the electrochemical solvent. In CH_3CN, fairly rapid degradation occurs (up to ~10% loss of electroactivity per cycle), which is due to the reactive nature of poly[(vbpy)Re-$(CO)_3]^-$.[3c] The wave shapes are diffusional in appearance. At a scan rate of 50 mV/s, the difference in oxidative and reductive peak potentials is $\Delta E_p \sim 200$ mV, which is due in part to the intrinsic resistivity of the OTE. However, at Pt or glassy-carbon electrodes the peak-to-peak splitting remains large (~150 mV). In film-based systems of this kind, the deviations from symmetrical, ideal surface waves with $\Delta E_p = 0$ are often a consequence of limiting self-exchange rates or of limited counterion mobility.[4b] In this case, the coupled chemical steps, i.e., metal–metal bond cleavage and re-formation, may also contribute to ΔE_p.

It is possible to estimate surface coverage by integration of the voltammetric response for the reoxidative portion of the second scan in Figure 1B (dashed line). From the integration, 2.6×10^{-8} mol/cm^2 of electrons were passed. From the stoichiometry, $2Re^- \rightarrow Re_2 + 2e^-$, the maximum surface coverage of poly[(vbpy)-$Re(CO)_3]_2$ is $\Gamma_{Re_2} = 1.3 \times 10^{-8}$ moles/cm^2. Spectroscopic evidence will be presented below, which suggests that nearly all of the Re sites in the film are, in fact, dimeric in nature.

Spectral Properties of the Films. The UV–visible spectra of the poly[(vbpy)$Re(CO)_3]_2$ film from Figure 1 before and after photolysis in the presence of CCl_4 are shown in Figure 2. As shown in Figure 2 and in Table I, the pattern of visible absorption bands that appear in poly[(vbpy)$Re(CO)_3]_2$ are in agreement with those that appear for the model compound, [(4,4′-dmbpy)Re-$(CO)_3]_2$ (4,4′-dmbpy is 4,4′-dimethyl-2,2′-bipyridine) in solution. The spectrum of [(4,4′-dmbpy)$Re(CO)_3]_2$ in CH_3CN includes absorption maxima at $\lambda_1 = 434$ nm ($\epsilon = 8900$ M^{-1} cm^{-1}), $\lambda_2 =$

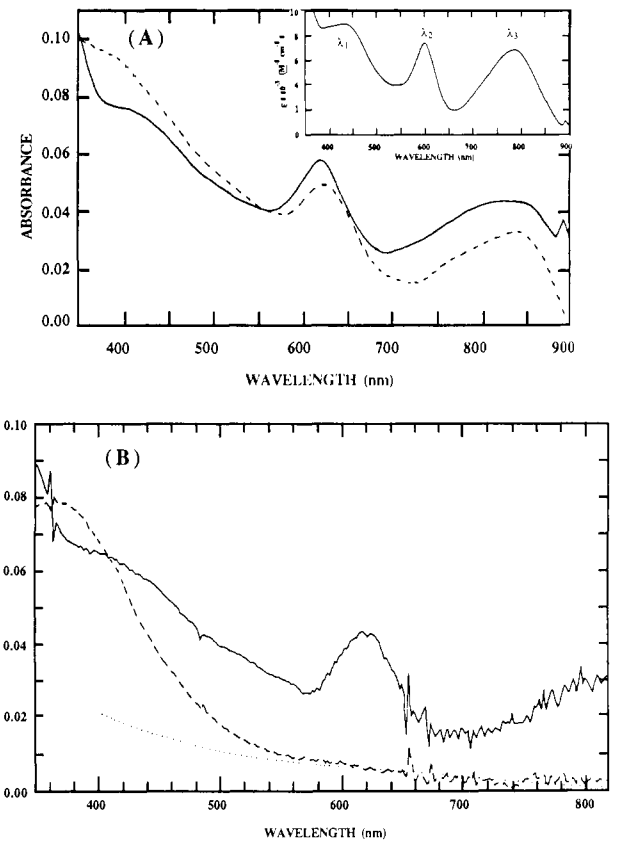

Figure 2. (A) UV–visible spectrum of the poly[(vbpy)$Re(CO)_3]_2$ film from Figure 1 with CH_3CN as the external solvent (—) and CCl_4 as the external solvent (- - -). (Inset) UV–visible spectrum of [(4,4′-dmbpy)-$Re(CO)_3]_2$ in CH_3CN. The spectra were obtained on a Cary 14 spectrophotometer. The apparent absorption feature at 890 nm is an instrumental artifact. (B) UV–visible spectrum of the poly[(vbpy)Re-$(CO)_3]_2$ film from Figure 1 in CH_3CN (—) and following photolysis in CCl_4 at 436 nm for 1 min (- - -). The dotted line (···) is the estimated base line arising from light-scattering effects (see the Experimental Section). The spectra were obtained by using a HP Model 8415A diode array spectrophotometer.

Table I. Electronic Absorption Spectral Maxima (±1 nm)

complex[a]	solvent	λ_1	λ_2	λ_3
[(bpy)$Re(CO)_3]_2$	CH_3CN	454	592	778
	CH_2Cl_2	472	608	806
[(4,4′-dmbpy)$Re(CO)_3]_2$	CH_3CN	434	596	786
	CH_2Cl_2	460	614	807
poly[(vbpy)$Re(CO)_3]_2$[b]	CH_3CN	~430	622	826
	CCl_4	c	630	845

[a] bpy is 2,2′-bipyridine; 4,4′-dmbpy is 4,4′-dimethyl-2,2′-bipyridine; vbpy is 4-methyl-4′-vinyl-2,2′-bipyridine. [b] As a polymeric film on an optically transparent, In-doped SnO_2 electrode immersed in the solvent indicated. [c] A discrete absorption maximum is not discernible.

596 nm ($\epsilon = 7300$ M^{-1} cm^{-1}), and $\lambda_3 = 786$ nm ($\epsilon = 6800$ M^{-1} cm^{-1}).

It is possible to use light absorbance measurements to estimate the Re_2 content of the films once corrections are made for the sloping backgrounds (Figure 2B). The backgrounds have their origin in wavelength-dependent light scattering (see the Experimental Section). By using eq 4 and the absorbance at 622 nm,

$$\Gamma_{Re_2}(1000 \text{ cm}^3/\text{dm}^3)\epsilon^{622} = A^{622} \quad (4)$$

the molar extinction coefficient for λ_2 of poly[(vbpy)$Re(CO)_3]_2$ with CH_3CN as the external solvent is calculated to be $\epsilon^{622} = 7100 \pm 700$ M^{-1} cm^{-1}. This value is in good agreement with $\epsilon^{596} = 7300$ M^{-1} cm^{-1} for λ_2 of [(4,4′-dmbpy)$Re(CO)_3]_2$ in CH_3CN. If a significant portion of the Re sites in the film had not dimerized, the calculated extinction coefficient would be considerably less than 7300 M^{-1} cm^{-1}.

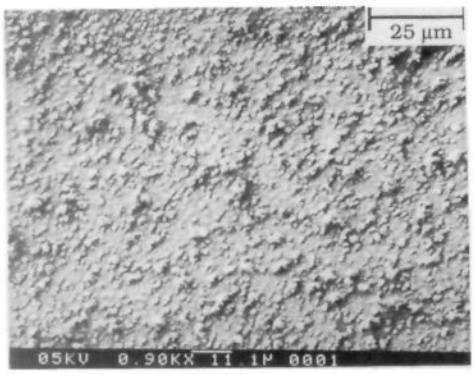

Figure 3. Scanning electron micrograph of a poly[(vbpy)Re(CO)$_3$]$_2$ film on a glassy-carbon electrode with $\Gamma_{Re_2} = 6 \times 10^{-8}$ mol/cm^2.

Indirect evidence supporting a high content of Re_2 within the films comes from electron microprobe X-ray fluorescence measurements. In the X-ray spectra, there is no evidence for fluorescence from either P or Cl although intense fluorescences appear for P at 2.01 keV in poly[(vbpy)Re(CO)$_3$S](PF$_6$) (S = solvent) and for Cl at 2.62 keV in poly[(vbpy)Re(CO)$_3$Cl]. A scanning electron micrograph of a thick film of poly[(vbpy)Re(CO)$_3$]$_2$ on carbon ($\Gamma_{Re_2} = 6 \times 10^{-8}$ mol/cm^2) is shown in Figure 3. The SEM reveals considerable surface roughness in the form of large polymeric particles, which are up to 5 μm in diameter. The particles are nucleated atop a smoother underlying film coating. The advent of the large surface particles under our conditions occurs at $\Gamma_{Re_2} \sim 1 \times 10^{-8}$ mol/cm^2.

Photochemistry. In the dark, films of poly[(vbpy)Re(CO)$_3$]$_2$ immersed in CCl_4 are stable for at least 5 days. When irradiated with near-UV or visible light out to 700 nm, the dark green color of the films quickly turns to yellow. The UV–visible spectra of photolyzed films (Figure 2B) match the spectrum of poly[(vbpy)Re(CO)$_3$Cl] with $\lambda_{max} = 380$ nm.[3] The photochemical transformation also occurs with CH_2Cl_2 as the external solvent but at a slower rate. The films are photochemically stable for at least 10 min when photolyzed with CH_3CN or DFB as the external solvent. Under the same conditions, there is no sign of photochemical reactivity toward CO_2 in CH_3CN (1 atm of CO_2, 0.14 M) or toward pure CH_3OH after 10 min of irradiation with filtered sunlight.

Photochemical kinetic studies in CCl_4 were conducted at excitation wavelengths of 436, 540, and 580 nm. The results obtained at 540 and 436 nm are shown in parts A and B of Figure 4, respectively, as plots of ln {Γ_{Re_2}} versus time. As discussed later, the results obtained at 436 nm are complicated by a secondary reaction involving reductive quenching of the metal-to-ligand charge-transfer (MLCT) excited state of the photolysis product, poly[(vbpy)Re(CO)$_3$Cl]. The MLCT excited state (eq 5a)

$$\text{poly}[(\text{vbpy})\text{Re}^{\text{I}}(\text{CO})_3\text{Cl}] \xrightarrow{h\nu} \text{poly}[(\text{vbpy}^{\bullet-})\text{Re}^{\text{II}}(\text{CO})_3\text{Cl}]^* \quad (5a)$$

is a powerful oxidant, $E^{0*/1-} \sim +1.15$ V vs ssce for [(phen)Re(CO)$_3$Cl].[8] In order to demonstrate the electron-transfer reactivity, a film of poly[(vbpy)Re(CO)$_3$Cl] ($\Gamma_{ReCl} \sim 5 \times 10^{-9}$ mol/cm^2) on a 0.1-cm^2 Pt electrode was photolyzed in an anaerobic CH_3CN solution containing 0.1 M TBAH and 0.25 M triethanolamine (TEOA). With potentiostating at +0.1 V and irradiation at 436 nm, an oxidative photocurrent of 10 μA/cm^2 was generated. The photocurrent arises by irreversible reductive quenching of the MLCT excited state[9] (eq 5b) followed by electron-transfer to the electrode (eq 5c). Significant photocurrents were not observed at bare Pt electrodes, in the absence of TEOA, or under 540- or 580-nm illumination.

$$\text{poly}[(\text{vbpy})\text{Re}(\text{CO})_3\text{Cl}]^* \xrightarrow{\text{TEOA}} \text{poly}[(\text{vbpy})\text{Re}(\text{CO})_3\text{Cl}]^- \quad (5b)$$

$$\text{poly}[(\text{vbpy})\text{Re}(\text{CO})_3\text{Cl}]^- \xrightarrow{-e^-} \text{poly}[(\text{vbpy})\text{Re}(\text{CO})_3\text{Cl}] \quad (5c)$$

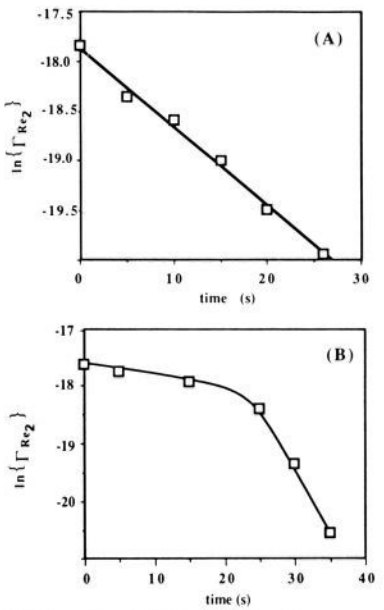

Figure 4. (A) Photochemical kinetics for the conversion of poly[(vbpy)Re(CO)$_3$]$_2$ to poly[(vbpy)Re(CO)$_3$Cl]. The film was immersed in CCl_4 and photolyzed at 540 nm ($I^\circ = 8.9 \times 10^{-8}$ einsteins/cm^2-s). The reaction was monitored at 630 nm. (B) As in (A) but with photolysis at 436 nm ($I^\circ = 3.9 \times 10^{-8}$ einsteins/cm^2-s).

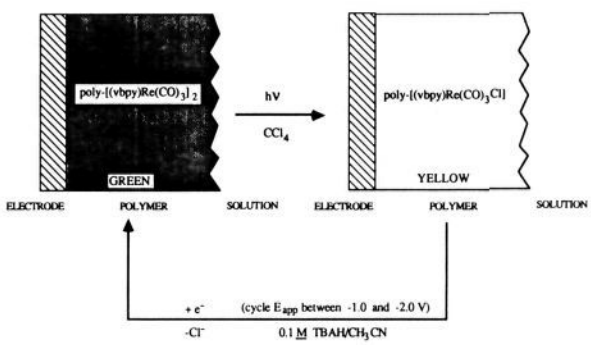

Figure 5. Schematic diagram illustrating the chemical basis for the photochemical–electrochemical write–erase cycle.

Imaging and Metal Deposition. It is the color difference between poly[(vbpy)Re(CO)$_3$Cl] and poly[(vbpy)Re(CO)$_3$]$_2$ that provides the basis for the photochemical–electrochemical write–erase cycle. When immersed in CCl_4 in a cell that has been masked with an appropriate pattern and photolyzed, a yellow image appears in the dark green background of the nonphotolyzed dimer. The yellow-on-green image can be erased electrochemically and the film restored to its original green color by twice cycling the potential of the electrode immersed in 0.1 M TBAH/DFB between −1.0 and −1.85 V. The cycle is illustrated schematically in Figure 5.

In a single write–erase cycle, 70% of the original absorbance at 630 nm due to poly[(vbpy)Re(CO)$_3$]$_2$ can be recovered. The regenerated film can be used again to form a new image, but, after a third exposure, the dimer is not regenerated by electrochemical cycling to any significant degree. At the end of three write–erase cycles, the film is yellow-orange. Infrared analysis shows a ν(CO) band at 2021 cm^{-1}, which is characteristic of *fac*-[(bpy)Re(CO)$_3$Cl], but other species are also present in small amounts,

(8) Luong, J. C.; Nadjo, L.; Wrighton, M. S. *J. Am. Chem. Soc.* **1978**, *100*, 5790.

(9) (a) Hawecker, F.; Lehn, J.-M.; Ziessel, R. *J. Chem. Soc., Chem. Commun.* **1982**, 536. (b) Kutal, C.; Weber, M. A.; Ferraudi, G.; Geiger, D. *Organometallics* **1985**, *4*, 2161.

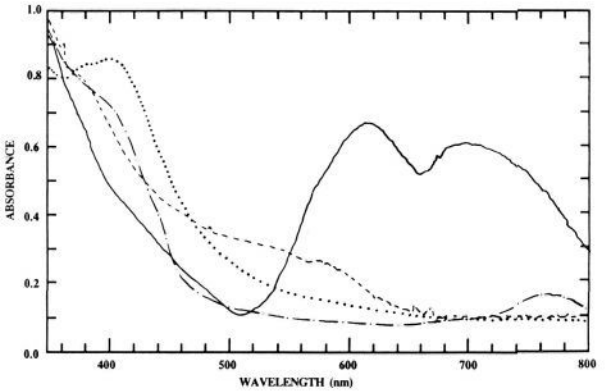

Figure 6. UV–visible spectra of films of poly[(vbpy)$Re(CO)_3]_2$ (of varying surface coverages) after immersion in acetonitrile solutions containing DDQ (---), TCNQ (-·-), $[Co(pc)(CH_3CN)_2]^+$ (—), and Ag^+ (···). The spectra were recorded by immersion of the film-coated electrodes in fresh CH_3CN after the reactions were complete.

with ν(CO) bands appearing at lower energy. Photolysis of poly[(vbpy)$Re(CO)_3]_2$ in CH_2Cl_2 instead of CCl_4 results in an orange-yellow film, which does not regenerate the dimer upon electrochemical cycling.

The dimer-containing films are oxygen sensitive. Their green color turns to yellow within minutes after exposure to air. In a photoimaging cycle, the loss of the green color destroys the contrast of the image with the background. The image can be permanently fixed by deliberate oxidation of nonphotolyzed Re_2 sites by using appropriate oxidants. For example, when films of poly[(vbpy)-$Re(CO)_3]_2$ are immersed in CH_3CN solutions containing TCNQ, DDQ, or $[Co(pc)(CH_3CN)_2]^+$, the color of the film changes to light green, orange-brown, and dark blue, respectively. Visible absorption bands appear in the films due to $TCNQ^-$, DDQ^-, or [Co(pc)], all of which remain in the film following the redox step (Figure 6). The light green color of the TCNQ-treated films turns to orange over a period of ~5 days while the colors of the other two are stable indefinitely. With TCNQ or $[Co(pc)-(CH_3CN)_2]^+$ as oxidants, poly[(vbpy)$Re(CO)_3]_2$ can be partially regenerated by reductive scans between −1.0 and −1.85 V in 0.1 M TBAH/CH_3CN. With DDQ, reductive generation does not occur. No thermal reaction or significant color change occurs between these oxidants and the yellow, poly[(vbpy)$Re(CO)_3Cl$] regions of the films.

An example of the development of a secondary image is shown in Figure 7. In the experiment, the photolysis procedure with masking was used to produce the initial yellow-on-green image, which appears as an arrow. The image was "fixed" by subsequent exposure to a solution containing $[Co(pc)(CH_3CN)_2]^+$. The image was generated on an ITO electrode, and the graininess is a consequence of uneven film formation on this surface. Smoother films can be grown on Pt or glassy-carbon electrodes, but the reflectivity of these electrodes makes the images more difficult to capture photographically.

The Re_2 sites in poly[(vbpy)$Re(CO)_3]_2$ are also oxidized by Ag^+ in CH_3CN. When exposed to Ag^+, the green color of the films changes to orange (Figure 6), and elemental Ag is deposited. Following the initial treatment with Ag^+, additional silver can be electrodeposited into the Ag^+-oxidized portions of the film by potentiostating the electrode at 0.0 V in a 0.1 M solution of TBAH/CH_3CN containing Ag^+. In photogenerated images that had been treated with Ag^+ after photolysis, electrochemical deposition occurs selectively into the nonphotolyzed areas. The chemical–electrochemical cycle, which is illustrated schematically in Figure 8, produces a brown surface, which possesses a metallic luster.

Once deposited, elemental silver cannot be removed from the film by electrochemical oxidation. A small oxidation wave does appear at $E_{p,a}$ = +0.3 V, but an oxidative scan past this wave fails to result in any significant change in the orange color of the film. The silver can be removed by chemical oxidation. When treated

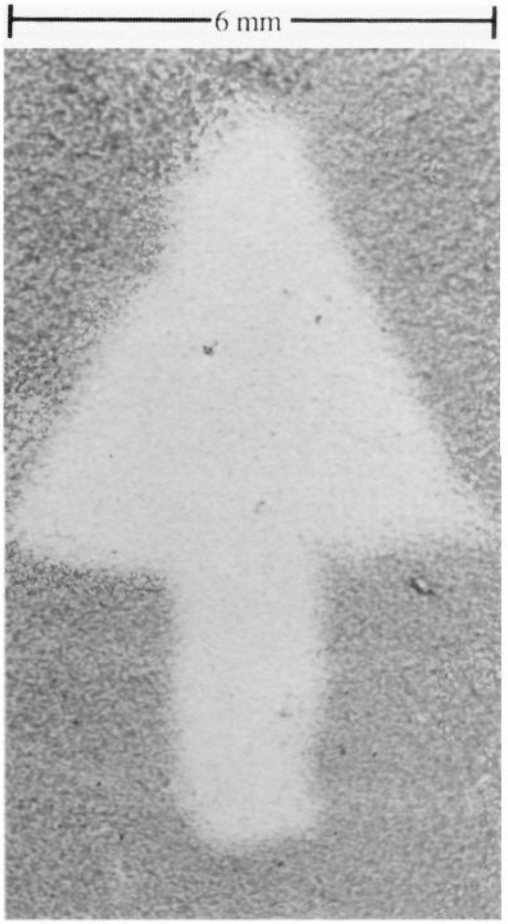

Figure 7. "Fixed" photoimage. The light area was produced by immersion and photolysis in CCl_4. The image was fixed by exposure to a solution containing $[Co(pc)(CH_3CN)_2]^+$.

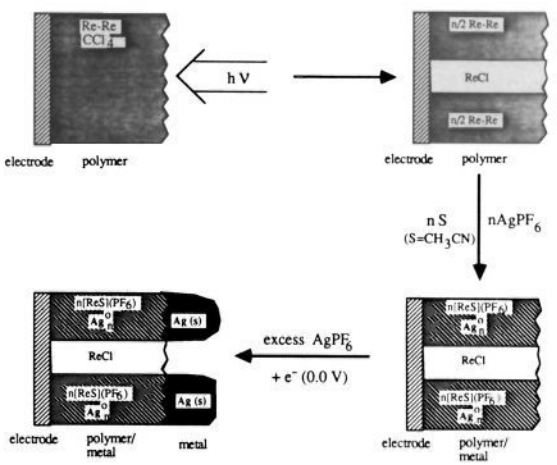

Figure 8. Photochemical–chemical–electrochemical cycle for spatially selective silver deposition in poly[(vbpy)$Re(CO)_3]_2$.

with Ce(IV) in CH_3CN, the orange film turns to the light yellow color of the acetonitrilo complex, poly[(vbpy)$Re(CO)_3(CH_3CN)]^+$.

Image Resolution. In order to test spatial resolution, a fine line pattern was generated by passing a laser beam through a diffraction grating as the photolysis source. A typical result is shown in the SEM in Figure 9. In the experiment, a poly[(vbpy)Re-$(CO)_3]_2$ film was photolyzed for 15 s in neat CCl_4 and fixed with $[Co(pc)(CH_3CN)_2]^+$. The lines in this case are ~15 μm wide and 40–50 μm apart. The blue color of Co(pc) was visible in the nonphotolyzed areas, but X-ray emission from Co was not sufficiently strong to be observed on the instrument available to us.

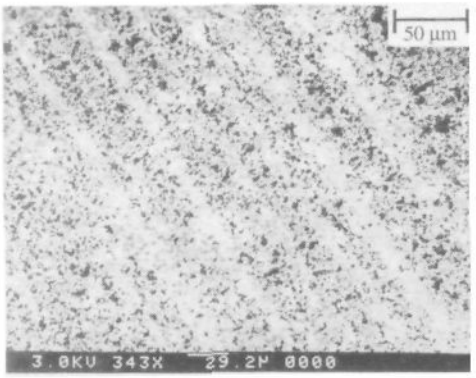

Figure 9. Scanning electron micrograph of a poly[(vbpy)$Re(CO)_3]_2$ film (2×10^{-8} mol/cm^2) on a platinum electrode that had been photolyzed for 15 s in CCl_4 and then treated with $[Co(pc)(CH_3CN)_2]^+$. The pattern was generated by laser photolysis (457.9 nm, 5 mW) through a diffraction grating. The lighter areas are the photolyzed regions.

X-ray fluorescence measurements show that Cl is present in both the dark and light areas in Figure 9 but that the Cl/Re ratio is significantly higher in the light (photolyzed) areas, as expected from the photochemistry.

Discussion

Photoimaging. The strategy that was chosen for the development of a photochemical–electrochemical write–erase cycle (eq 6 and 7 and Figure 5) has proven to be successful, at least in

$$\text{poly[(vbpy)Re(CO)}_3\text{]}_2 \xrightarrow{h\nu,\ CCl_4} 2\text{poly[(vbpy)Re(CO)}_3\text{Cl]} \quad (6)$$

$$2\text{poly[(vbpy)Re(CO)}_3\text{Cl]} \xrightarrow{+2e^-,\ -2Cl^-} \text{poly[(vbpy)Re(CO)}_3\text{]}_2 \quad (7)$$

concept. The photochemical reactivity of the metal–metal bond toward halocarbons is retained in the polymeric film environment. That reactivity combined with the reductive electrochemistry that returns poly[(vbpy)$Re(CO)_3$Cl] to the metal–metal bond completes the cycle.

The system is photochemically responsive to irradiation throughout the near-UV and visible spectra, but there are serious limitations to its use: (1) The unreacted dimeric sites are O_2 sensitive. (2) There is a 30% loss in regeneration ability with each write–erase cycle. Since the films are stable toward electrochemical cycling, deactivation must occur in the photolysis step. It probably arises by the formation of chemical sites in the films which appear following the scavenging of $CCl_3^\bullet$. Photochemically induced loss of CO[2] is apparently not a problem since the films are otherwise stable toward photolysis for periods of up to 10 min with CH_3CN as the external solvent. (3) The surface roughness and light-scattering properties of the films appear to limit the resolution of the imaging step. Nevertheless, it is possible to create structures on the tens of a micron scale without difficulty.

We have found that it is possible to develop and stabilize the photoimage by using the chemical oxidants TCNQ, DDQ, or $[Co^{III}(pc)(CH_3CN)_2]^+$ to oxidize unreacted poly[(vbpy)Re-$(CO)_3]_2$. The $TCNQ^-$ and DDQ^- anions are retained in the films by ion pairing or, perhaps, by binding to Re(I) via the cyano groups. $[Co^{II}(pc)]$ is insoluble in acetonitrile and appears to precipitate within the film following electron transfer. The most interesting chemistry of this kind has appeared with Ag^+ as the oxidant. The oxidation proceeds with the formation of elemental silver, probably as small clusters (eq 8). A new, intense absorption feature appears at $\lambda_{max} = 405$ nm, which may arise from an intracluster transition[10] or, perhaps, from a new MLCT transition.

$$n\text{Ag}^+ + \frac{n}{2}\text{poly[(vbpy)Re(CO)}_3\text{]}_2 + n\text{CH}_3\text{CN} \rightarrow \text{Ag}^0_n + n\text{poly[(vbpy)Re(CO)}_3\text{(CH}_3\text{CN)]}^+ \quad (8)$$

(10) Ozin, G. A.; Huber, H. *Inorg. Chem.* **1978**, *17*, 155.

The unsuccessful attempts to reoxidize Ag^0_n to nAg$^+$ electrochemically suggest that the silver clusters must be dispersed throughout the films. A small oxidation wave is observed on an initial oxidative scan but accounts for less than 10% of the total silver content. Apparently, electrochemical reoxidation can occur, but only for those particles in the film that are at or near the electrode/film interface. Following the oxidation of those particles, the electron-transfer chain to the electrode is broken (eq 9) and further oxidation inhibited.

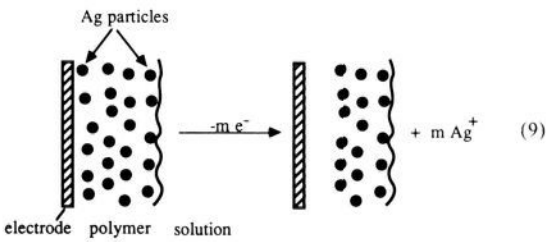

(9)

For Ag^+-treated films, which have not undergone electrochemical oxidation, electron-transfer channels between the Ag^0_n clusters and the electrode do exist, as shown by the successful electrochemical deposition of silver. At the electrolysis potential used, 0.0 V, Ag^+ is slowly reduced to Ag metal at a bare OTE under the same conditions. In the polymeric films, rapid deposition occurs, but only in those regions that contain the Ag^0_n clusters that were formed from the oxidation of Re_2 by Ag^+. By inference, electron transfer occurs from the electrode to clusters near the electrode and then to clusters throughout the film. The ability of Ag^0 to deposit within the films requires the existence of an electron-transfer channel from the electrode to the polymer/solution interface and the presence of the preformed Ag^0_n clusters to act as nucleation sites for facilitating particle growth.

The photochemical/electrochemical sequence used for Ag metal deposition is illustrated schematically in Figure 8. We regard this sequence and the ability to build spatially defined structures as potentially one of the most interesting observations that we have made. Reaction sequences of this kind hold promise for the fabrication of controlled microstructures within the polymeric film environment.

Photochemical Mechanism. A second theme of interest to us in this work was the establishment of the mechanistic details by which the metal–metal bond photochemistry occurs within the films. Mechanistic studies in solution[1,2,11-13] have shown that the photochemistry proceeds via intermediates, which arise either from homolytic cleavage, e.g., $Mn(CO)_5^\bullet$ (eq 1) or loss of CO, e.g., $Mn_2(CO)_9$ from $Mn_2(CO)_{10}$. The 17e monomers such as Mn-$(CO)_5^\bullet$ undergo halogen atom abstraction reactions with halocarbons. They are followed by coupling and related reactions of the organic radical.

There are some interesting questions that arise for the film-based photochemistry. Do the same photochemical pathways appear in the films as in solution? Can evidence be found for collective effects involving more than one Re_2 site given their high density and close proximity within the films?

Before turning to mechanism it is useful to consider the physical and electronic state of the Re_2 sites within the films. Given the

(11) (a) Hughey, J. L.; Anderson, C. P.; Meyer, T. J. *J. Organomet. Chem.* **1977**, *125*, C49. (b) Kidd, D. R.; Brown, T. L. *J. Am. Chem. Soc.* **1978**, *100*, 4095. (c) Fox, A.; Poë, A. *J. Am. Chem. Soc.* **1980**, *102*, 2497. (d) Wegman, R. W.; Olsen, R. J.; Gard, D. R.; Faulkner, L. R.; Brown, T. L. *J. Am. Chem. Soc.* **1981**, *103*, 6089. (e) Yesaka, H.; Kobayashi, T.; Yasufuku, K.; Nagakura, S. *J. Am. Chem. Soc.* **1983**, *105*, 6249. (f) Stiegman, A. E.; Tyler, D. R. *Inorg. Chem.* **1984**, *23*, 527. (g) Stiegman, A. E.; Goldman, A. S.; Philbin, C. E.; Tyler, D. R. *Inorg. Chem.* **1986**, *25*, 2976. (h) Prinslow, D. A.; Vaida, V. *J. Am. Chem. Soc.* **1987**, *109*, 5097. (i) Firth, S.; Klotzbucher, W. E.; Poliakoff, M.; Turner, J. J. *Inorg. Chem.* **1987**, *26*, 3370.

(12) (a) Giannoti, C.; Merle, G. *J. Organomet. Chem.* **1976**, *105*, 97. (b) Abrahamson, H. B.; Palazotto, M. C.; Reichel, C. L.; Wrighton, M. S. *J. Am. Chem. Soc.* **1979**, *101*, 4123. (c) Tyler, D. R.; Schmidt, M. A.; Gray, H. B. *J. Am. Chem. Soc.* **1983**, *105*, 6018.

(13) (a) Wrighton, M. S.; Ginley, D. S. *J. Am. Chem. Soc.* **1975**, *97*, 4246. (b) Laine, R. M.; Ford, P. C. *Inorg. Chem.* **1977**, *16*, 388.

facile reduction of poly[(vbpy)Re(CO)$_3$Cl] to poly[(vbpy)Re(CO)$_3$]$_2$, there must be considerable motional flexibility within the films in order to allow for Cl$^-$ loss and subsequent Re–Re bond formation. The Re–Re coupling may involve sites on separate polymeric strands (eq 10a), adjacent sites along the same polymeric strand (eq 10b), or coupling of both types.

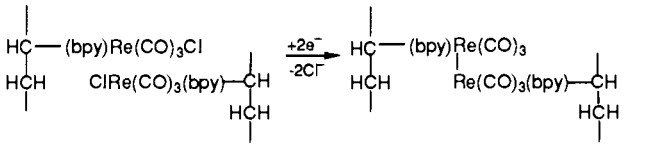

(10a)

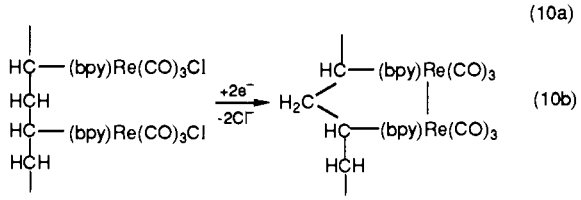

(10b)

The similarities in the patterns of absorption bands that appear in the electronic spectra of [(4,4′-dmbpy)Re(CO)$_3$]$_2$ and poly[(vbpy)Re(CO)$_3$]$_2$ suggest that the electronic structure and facial geometry at Re are maintained in the films. Given their intensities and medium dependences (Table I), the three visible absorption bands probably have a charge-transfer origin. Wrighton and Morse[14a] have assigned the lowest energy absorption band in (phen)(CO)$_3$ReRe(CO)$_5$ to a σ(Re–Re) → π^*(bpy) charge-transfer transition. From cyclic voltammetric measurements on [(bpy)Re(CO)$_3$]$_2$ in 1,2-difluorobenzene,[6] there is a 1.43-V difference between 1e oxidation at σ(Re–Re) ($E_{1/2}$ = −0.12 V) and 1e reduction at the lowest π^*(bpy) level ($E_{1/2}$ = −1.55 V). Given this energy difference of 11 500 cm^{-1} (870 nm), the assignment of the lowest energy absorption band, λ_3 to a σ(Re–Re) → π^*(bpy) transition is reasonable, at least energetically. In any case, the visible charge-transfer transitions apparently act as efficient intramolecular sensitizers of a low-lying $\sigma\sigma^*$(Re–Re) state, which, when populated, leads to homolysis of the Re–Re bond.[2]

The absorption spectra of the films also give insight into the immediate environment that surrounds the Re$_2$ sites. As found for (phen)(CO)$_3$ReRe(CO)$_5$[14a] and complexes of the type [(bpy)Re(CO)$_3$L]$^{n+}$,[14b] absorption maxima for the Re$_2$ dimers are medium dependent (Table I). Less polar solvents cause a shift to lower energy for all three of the visible transitions. The decrease in energy arises because there is a decrease in the dipole moment of the MLCT excited state compared to the ground state. The shift to lower energy in λ_2 of 700 cm^{-1} for poly[(vbpy)Re(CO)$_3$]$_2$ compared to [(4,4′-dmbpy)Re(CO)$_3$]$_2$ in CH$_3$CN suggests that the Re$_2$ sites find themselves in a relatively nonpolar environment in the films. There is a further shift of λ_2 and λ_3 to lower energies (−200 and −270 cm^{-1}, respectively) with CCl$_4$ as the external solvent compared to CH$_3$CN. There is a far more pronounced shift between CH$_3$CN and CH$_2$Cl$_2$, which is more polar than CCl$_4$, for the dimers in solution (Table I). We conclude from the spectral data that the films must be somewhat swollen with solvent but that the environment surrounding the Re$_2$ sites in the films is governed largely by the polymeric matrix itself. Solvent molecules are certainly present in the films given the spectral results and the photochemical reaction with CCl$_4$. However, in terms of composition, the solvent does not dominate the properties of the interior environment as it would for an isolated molecule in solution.

Photochemical Kinetics. Irradiation at 540 nm. From the data in Figure 4A, irradiation of films of poly[(vbpy)Re(CO)$_3$]$_2$ at 540 nm leads to a linear decrease in ln {Γ_{Re_2}} with photolysis time. The first-order nature of the decay using 540-nm radiation is consistent with the series of reactions shown in Scheme I. These reactions

Scheme I. 540-nm Irradiation

$$Re_2 \underset{1/\tau_{Re_2}^*}{\overset{h\nu}{\rightleftharpoons}} Re_2^* \xrightarrow{k_1} [Re^\bullet, Re^\bullet] \qquad (11)$$

(k_b)

$$[Re^\bullet, Re^\bullet] + 2CCl_4 \xrightarrow{k_2} 2ReCl \qquad (12)$$

are taken from well-established mechanisms proposed for homolytic M–M bond cleavage in solution.[1,2,11-13] In Scheme I, Re$_2$ is poly[(vbpy)Re(CO)$_3$]$_2$, [Re$^\bullet$,$^\bullet$Re] is the radical pair poly[(vbpy)(CO)$_3$Re$^\bullet$,$^\bullet$Re(CO)$_3$(vbpy)], and ReCl is poly[(vbpy)Re(CO)$_3$Cl]. In eq 11, τ_{Re_2} is the excited-state lifetime, k_1 is the rate constant for homolytic cleavage, and k_b is the rate constant for recombination of the radical pair. In eq 12, k_2 is the rate constant for the halogen atom abstraction reaction. There is no observable emission from the dimer at room temperature either in solution or in the films showing that τ_{Re_2}* is dominated by nonradiative processes.

In an attempt to account for the time-dependent data quantitatively, we have developed a kinetic model based on the reactions in Scheme I. In the analysis, recombination (k_b, eq 11) is treated as a first-order process rather than as a second-order process. The basis for this assumption is the loss of translational mobility upon binding to the polymer. Once formed, the polymer-bound 17e rhenium radicals cannot separate. Because the intensity of the incident radiation in the photochemical experiments was relatively low, the steady-state concentration of excited states and of radical pairs is low as well. Assuming that there is no exchange between sites via Re$^\bullet$ + Re$_2$ → Re$_2$ + Re$^\bullet$, a photogenerated Re$^\bullet$ site should only be able to recombine with its original photogenerated partner or to react with CCl$_4$. There is no diffusional component to the recombination process. Kinetically, the first-order assumption is equivalent to regarding the pair of photochemically produced monomers as a high-energy isomer of the metal–metal bonded dimer, which "decays" to the ground state by first-order kinetics.

If it is further assumed that the reaction between Re$^\bullet$ and CCl$_4$ is pseudo-first-order in CCl$_4$, application of the steady-state approximation to [Re$_2$*] and [Re$^\bullet$,$^\bullet$Re], integration, and conversion to surface coverage units (Appendix) leads to eq 13. In eq 13,

$$\ln \{\Gamma_{Re_2}\} = -2.303 I^\circ(\epsilon_{Re_2}{}^{540})1000\phi t + \ln \{\Gamma_{Re_2}{}^\circ\} \qquad (13)$$

$$\phi = \eta^{540}\left\{1 - \frac{1/\tau_{Re_2^*}}{1/\tau_{Re_2^*} + k_1} - \frac{k_b k_1}{(k_b + 2k_2[CCl_4])(1/\tau_{Re_2^*} + k_1)}\right\} \qquad (14)$$

$\Gamma_{Re_2}{}^\circ$ is the initial surface coverage of poly[(vbpy)Re(CO)$_3$]$_2$, Γ_{Re_2} is the surface coverage at time t, I° is the light intensity at 540 nm (einsteins/s·cm^2), η^{540} is the efficiency with which the Re$_2$* state is reached following excitation at 540 nm, and ϕ is the fraction of photochemical events that convert Re$_2$ into ReCl. It is defined in eq 14.

Equation 13 correctly predicts the linear relationship between ln {Γ_{Re_2}} and t that appears for irradiation at 540, Figure 4A. From the experimental slope of 0.79, I° (=8.9 × 10^{-8} einsteins/s·cm^{-2}), and ϵ (=3800 M^{-1} cm^{-1}), ϕ = 0.11. Similar results were obtained upon photolysis at 580 nm. In two repetitive experiments, values of ϕ = 0.06 and 0.17 were obtained for an average value of ϕ = 0.1. By comparison, disappearance quantum yields for the photochemical reactions of M–M bonded dimers in CH$_2$Cl$_2$/CCl$_4$ mixtures are typically 0.1 or above.[1,2,11-13] A significant contribution to the variations observed in ϕ between the films in different experiments may come from differences in their light-scattering properties.

Irradiation at 436 nm. From the plot in Figure 4B, the loss of Re$_2$ upon photolysis at 436 nm not only does not follow simple first-order kinetics but the rate actually *increases* with photolysis time. There is *no* wavelength dependence in the solution photochemistry of the model compound [(4,4′-dmbpy)Re(CO)$_3$]$_2$. In CH$_2$Cl$_2$, the disappearance of this dimer occurs by first-order kinetics with ϕ(580 nm) = 0.011 and ϕ(436 nm) = 0.010. The

(14) (a) Morse, D. L.; Wrighton, M. S. *J. Am. Chem. Soc.* **1976**, *98*, 3931. (b) Kalyanasundaram, K. *J. Chem. Soc., Faraday Trans. 2* **1986**, *82*, 2401. (c) Kaim, W.; Kohlmann, S.; Ernst, S.; Olbrich-Deussner, B.; Bessenbacher, C.; Schulz, A. *J. Organomet. Chem.* **1987**, *321*, 215.

contrast in behavior between the two irradiation wavelengths in the films suggests that the photolysis product, poly[(vbpy)Re(CO)$_3$Cl], is involved in the photochemistry at 436 nm. Although poly[(vbpy)Re(CO)$_3$Cl] does not absorb light appreciably at 540 or 580 nm, it is a significant light absorber at 436 nm.

There are two ways that the photoproduct could enter into the mechanism. One is by energy-transfer sensitization of Re_2* by the MLCT state of poly[(vbpy)Re(CO)$_3$Cl] (eq 15 and 16). The

$$\mathrm{ReCl} \underset{1/\tau_{\mathrm{ReCl}^*}}{\overset{h\nu}{\rightleftharpoons}} \mathrm{ReCl}^* \qquad (15)$$

$$\mathrm{ReCl}^* + \mathrm{Re_2} \rightarrow \mathrm{ReCl} + \mathrm{Re_2}^* \qquad (16)$$

second is by utilization of the oxidizing character of the ReCl* MLCT excited state toward adjacent Re_2 sites in the first of a series of reactions (eq 17a–c) that would lead to net halogen abstraction. The oxidative properties of poly[(vbpy)Re(CO)$_3$Cl]* toward triethanolamine provided the basis for the photoelectrochemical sequence in eq 4a–c. Poly[(vbpy)Re(CO)$_3$]$_2$ is a better reducing agent (E_{pa} = –0.15 V in CH_3CN) than is triethanolamine by ~1 V.

$$\mathrm{ReCl}^* + \mathrm{Re_2} \rightarrow [\mathrm{ReCl}]^- + [\mathrm{Re\cdots Re}]^+ \qquad (17a)$$

$$[\mathrm{Re\cdots Re}]^+ \rightarrow \mathrm{Re}^\bullet + \mathrm{Re}^+ \qquad (17b)$$

$$\mathrm{Re}^+ + [\mathrm{ReCl}]^- \rightarrow \mathrm{Re}^\bullet + \mathrm{ReCl} \qquad (17c)$$

We were unable to obtain satisfactory quantitative kinetics data at 436 nm. The individual data points were scattered and the extent of curvature in the ln $\{\Gamma_{Re_2}\}$ vs t plots varied significantly from run to run. However, the increase in rate with time shows that the pathway involving poly[(vbpy)Re(CO)$_3$Cl]* must occur with a relatively high efficiency.

Photochemistry in Thin Polymeric Films. Our results show that the Re–Re bond-based photochemistry of [(bpy)Re(CO)$_3$]$_2$ is retained in poly[(vbpy)Re(CO)$_3$]$_2$, and that the MLCT-based photochemistry of [(bpy)Re(CO)$_3$Cl] also appears in poly[(vbpy)Re(CO)$_3$Cl]. In addition, new pathways can appear in the condensed, concentrated environment of the films. This is illustrated by the photolysis of poly[(vbpy)Re(CO)$_3$]$_2$ at 436 nm in the presence of CCl_4. Under these conditions, the combination of the Re–Re bond-based photochemistry of poly[(vbpy)Re(CO)$_3$]$_2$ and the MLCT-based photochemistry of poly[(vbpy)Re(CO)$_3$Cl] leads to an additional, uniquely film-based photochemical pathway. The appearance of the additional pathway relies upon both complexes being present and held in close proximity.

The film environment also influences the kinetic details of the individual steps in the photochemical mechanisms. The interiors of the films are nonpolar and not highly swollen with solvent. They do allow for the facile translational diffusion of small molecules such as CCl_4 to reactive sites following excitation. The translational motion of the photogenerated 17e monomers, poly[(vbpy)Re(CO)$_3$•], is restricted because they are chemically bound and part of the polymer backbone. Once separated monomers are formed in solution, recombination is diffusional in nature, and its time scale is relatively slow, ~10–100 μs for a typical solution experiment.[2] This gives them an extended opportunity to encounter and undergo a reaction with a potential substrate. Recombination is far more rapid in the films because the monomers cannot separate, and recombination is a first-order process. Because of a far shorter recombination time scale, photochemical reactions can only occur with very reactive substrates, which concentrate in and diffuse freely through the films. This explains, for example, why photochemical reactions between poly[(vbpy)Re(CO)$_3$]$_2$ and CO_2 in CH_3CN or with alcohols do not occur even though both are substrates for [(bpy)Re(CO)$_3$•] generated either photochemically or electrochemically.

Acknowledgment. We acknowledge the Gas Research Institute for financial support of this research, Jill Rickman for obtaining SEM results, and Bob Kessler for assistance with the laser optics.

Appendix. Derivation of the Rate Law for Photolysis at 540 nm

On the basis of the mechanism in Scheme I, the rate of disappearance of Re_2 is given by eq A.1. The first term in eq A.1

$$\frac{-\mathrm{d}[\mathrm{Re_2}]}{\mathrm{d}t} = \eta^{540} I^\circ [1 + 10^{-A_{Re2}}] - (1/\tau_{\mathrm{Re_2}^*})[\mathrm{Re_2}^*] - k_b[\mathrm{Re}^\bullet,\mathrm{Re}^\bullet] \qquad (A.1)$$

is the rate of formation of the initial excited state by light absorption (eq A.2). In eq A.2, I° is the light intensity at 540 nm in einsteins/dm^3·s, $\epsilon_{Re_2}{}^{540}$ is the molar extinction coefficient for Re_2 at 540 nm in M^{-1} cm^{-1}, and η^{540} is the efficiency with which Re_2* is formed following excitation at 540 nm. A_{Re_2} is the absorbance of poly[(vbpy)Re(CO)$_3$]$_2$ at the excitation wavelength (eq A.3). It is sufficiently low (<0.05) in the films to justify the approximation in eq A.2. Equation A.2 describes the rate of

$$\frac{\mathrm{d}[\mathrm{Re_2}^*]}{\mathrm{d}t} = \eta^{540} I^\circ [1 - 10^{-A_{Re2}}] \approx \eta^{540} 2.303 I^\circ A_{\mathrm{Re_2}} \qquad (A.2)$$

$$A_{\mathrm{Re_2}} = (\epsilon_{\mathrm{Re_2}}{}^{540}) b [\mathrm{Re_2}] \qquad (A.3)$$

formation of the initial excited states by light absorption.

Applying the steady-state approximation to [Re_2*] and to [Re•,Re•] gives eq A.4 and A.5. Substitution of these equations

$$[\mathrm{Re_2}^*] = \frac{\eta^{540} 2.303 I^\circ (\epsilon_{\mathrm{Re_2}}{}^{540}) b [\mathrm{Re_2}]}{1/\tau_{\mathrm{Re_2}^*} + k_1} \qquad (A.4)$$

$$[\mathrm{Re}^\bullet,\mathrm{Re}^\bullet] = \frac{k_1 [\mathrm{Re_2}^*]}{k_b + 2k_2[\mathrm{CCl_4}]} \qquad (A.5)$$

into eq A.1 yields eq A.6.

$$\frac{-\mathrm{d}[\mathrm{Re_2}]}{\mathrm{d}t} = 2.303 I^\circ (\epsilon_{\mathrm{Re_2}}{}^{540}) b [\mathrm{Re_2}] \phi_1 \qquad (A.6)$$

The constant ϕ in eq A.6 is defined in eq A.7.

$$\phi = \eta^{540}\left\{1 - \frac{1/\tau_{\mathrm{Re_2}^*}}{1/\tau_{\mathrm{Re_2}^*} + k_1} - \frac{k_b k_1}{(k_b + 2k_2[\mathrm{CCl_4}])(1/\tau_{\mathrm{Re_2}^*} + k_1)}\right\} \qquad (A.7)$$

In integrated form, eq A.6 becomes eq A.8 where $[Re_2]_0$ is the initial concentration of Re_2. Equation 13 results from eq A.8

$$\ln [\mathrm{Re_2}] = -2.303 I^\circ (\epsilon_{\mathrm{Re_2}}{}^{540}) b \phi t + \ln [\mathrm{Re_2}]_0 \qquad (A.8)$$

when the relationship between concentration, surface coverage (Γ_{Re_2} (in mol/cm^2)), and the film thickness, b (in cm), in eq A.9 is included.

$$[\mathrm{Re_2}] = \Gamma_{\mathrm{Re_2}} (1000\ \mathrm{cm^3/dm^3})/b \qquad (A.9)$$

(15) O'Toole, T. R., unpublished results.